Eduvest – Journal of Universal Studies
Volume 6 Number 7, July, 2026
p- ISSN 2775-3735- e-ISSN 2775-3727

The Role of LNG Regasification in Reducing Fuel Oil Consumption and Improving the Reliability of the Tarakan Isolated Power System: A Monte Carlo Simulation Approach

Ghusaebi*, Tri Wahyu Adi
Institut Teknologi Perusahaan Listrik Negara, Indonesia
Email: ghusaebi2410709@itpln.ac.id*, triwahyuadi@itpln.ac.id

Keywords
LNG regasification; fuel oil consumption; isolated power system; Loss of Load Probability; Monte Carlo simulation.

ABSTRACT
The Tarakan Power System is an isolated power system that relies on local generating units and primary energy resources. Its dependence on fuel oil-fired generation presents challenges to operational efficiency, while fluctuations in natural gas supply, peak demand, and generation availability affect system adequacy. This study evaluated the role of liquefied natural gas (LNG) regasification in reducing fuel oil consumption and improving system reliability. A data-driven Monte Carlo simulation compared a baseline scenario without LNG regasification with an intervention scenario incorporating conditional LNG supply. The stochastic input variables included pipeline natural gas supply, peak demand, and the available capacities of diesel and gas-engine power plants. Common Random Numbers (CRN) were applied to compare the two scenarios under identical stochastic conditions across 10,000 simulation iterations. Model validation yielded a coefficient of determination (R^2) of 0.8311 and a Mean Absolute Percentage Error (MAPE) of 11.23% for the fuel oil consumption model. The available-capacity model achieved a MAPE of 2.29%, while the operating status predicted from its estimates was classified with an accuracy of 98.95%. LNG regasification reduced average fuel oil consumption from 133.33 to 113.51 kL/day, representing a decrease of 19.82 kL/day (14.87%). It also increased the average available generation capacity from 60.94 to 64.02 MW and the reserve margin from 11.73 to 14.81 MW, while reducing the Loss of Load Probability (LOLP) from 2.26% to 0.21%. These findings indicate that conditional LNG regasification can function as a primary energy buffer and a source of operational flexibility, thereby reducing dependence on fuel oil and improving generation adequacy and reliability in the Tarakan isolated power system.

INTRODUCTION

Isolated power systems operate independently of larger interconnected grids and therefore rely entirely on local generating units and locally available primary energy resources. The absence of interconnection limits their ability to import electricity during generation shortages, making system reliability highly dependent on generation availability, fuel supply continuity, and load variability. Previous studies on isolated and stand-alone microgrids have shown that uncertainties in generation, equipment availability, weather conditions, and electricity demand can substantially affect resource adequacy and the probability of supply shortages (Nallainathan et al., 2025; Saleem & AlMuhaini, 2021; Weng et al., 2022). These characteristics make isolated power systems particularly vulnerable when their generation mix depends on fuel sources whose availability and operating conditions fluctuate over time.

The Tarakan Power System in North Kalimantan, Indonesia, is an isolated power system supplied primarily by diesel power plants, locally referred to as Pembangkit Listrik Tenaga Diesel (PLTD), and gas-engine power plants, referred to as Pembangkit Listrik Tenaga Mesin Gas (PLTMG). Diesel-fired generation provides operational flexibility but also creates continued dependence on fuel oil, with implications for operating efficiency and generation costs. Fuel prices and fuel consumption have been shown to be closely associated with operating costs, electricity production, and the operating income of electric utilities, emphasizing the importance of fuel management in power generation operations (Adi, 2023). Increasing the utilization of gas-fired generation may reduce fuel oil consumption; however, its contribution depends not only on the volume of natural gas supplied but also on the availability of PLTMG units and their ability to utilize the available gas.

Liquefied natural gas (LNG) regasification provides an additional source of gaseous fuel that can complement pipeline natural gas and support greater utilization of gas-fired generating units. In this context, LNG is not intended to permanently replace pipeline natural gas but rather to serve as a primary energy buffer when pipeline supply is insufficient. Constraints and congestion in natural gas networks can restrict the output of gas-fired generating units and may ultimately contribute to load shedding within the associated power system (Lai et al., 2021). LNG also offers flexibility in transportation and storage, making it particularly suitable for remote and island regions with limited access to conventional natural gas infrastructure (Zhang et al., 2024). Furthermore, flexibility in natural gas supply systems can improve the ability of integrated electricity and natural gas systems to respond to uncertainties in both supply and demand (Yang et al., 2026). For the Tarakan Power System, regasified LNG may facilitate fuel switching from oil-fired to gas-fired generation, provided that sufficient PLTMG capacity is available to utilize the additional gas.

The operational effects of LNG regasification cannot be adequately assessed using deterministic comparisons based solely on average operating conditions. Pipeline natural gas supply, peak demand, PLTD available capacity, and PLTMG available capacity vary over time and may interact to produce substantially different operating conditions. A reduction in natural gas supply can constrain gas-fired generation, reduce the operating reserve margin, and increase the likelihood of a generation deficit. More generally, uncertainty in power systems requires analytical approaches capable of representing the range and probability of possible operating conditions rather than producing only a single expected outcome (Singh et al., 2022). This requirement is particularly important in resource adequacy analysis, which evaluates whether available generation capacity can reliably meet electricity demand under uncertain conditions. Probabilistic reliability indices such as Loss of Load Probability (LOLP) provide a more informative representation of supply risk than deterministic reserve measures alone (Tillmanns et al., 2026).

Monte Carlo simulation is widely used in power system analysis because it can generate numerous combinations of uncertain input variables and estimate the probability distributions of system outputs. This approach enables the evaluation of expected operating conditions, extreme outcomes, and the probability of specific events, such as generation deficits (Abud et al., 2023). Previous reliability studies have applied Monte Carlo-based methods to isolated microgrids, renewable energy systems, equipment outages, and generation adequacy. However, most of these studies have focused on component reliability, renewable energy variability, energy storage operation, or general adequacy assessment rather than on the operational effects of a conditional LNG supply intervention. Consequently, relatively few studies have directly examined how additional regasified LNG interacts with gas utilization, aggregate daily fuel oil consumption, available generation capacity, reserve margin, operating status, and LOLP in an isolated power system dominated by diesel and gas-engine generation.

Research on small-scale LNG implementation in the Indonesian archipelago has primarily emphasized economic feasibility, diesel-fuel substitution, transportation, and supply-chain risk. Sommeng et al. (2023) demonstrated that small-scale LNG can provide a technically and economically viable alternative to diesel fuel for electricity generation in island regions. Other studies have shown that LNG implementation must account for maritime logistics, receiving-terminal limitations, transportation capacity, demand uncertainty, and operational risks throughout the supply chain (Machfudiyanto, Humang, et al., 2023; Machfudiyanto, Muslim, et al., 2023). Although these studies established the potential of LNG to support diesel-reduction programs, relatively little attention has been given to the operational behavior of LNG after it enters the power system and undergoes regasification. In particular, an increase in natural gas supply does not automatically reduce fuel oil consumption when PLTMG units are unavailable, derated, or unable to utilize the supplied gas.

The novelty of this study lies in the development of an integrated, data-driven probabilistic framework to evaluate the role of LNG regasification in an isolated power system. This framework extends beyond conventional before-and-after comparisons and stochastic analyses of individual system components by integrating an empirical fuel oil consumption model, a fuel-constrained available-capacity model, and a conditional LNG intervention model. Furthermore, it applies Common Random Numbers (CRN) to ensure a controlled ceteris paribus comparison, allowing the effects of the intervention to be distinguished from unrelated random variation. This methodological approach is novel because it simultaneously considers the stochastic characteristics of system inputs and the conditional operational behavior of LNG supply, thereby providing a more realistic assessment of LNG regasification as a primary energy buffer and source of operational flexibility.

This study addressed this research gap by developing an integrated, data-driven probabilistic framework to evaluate LNG regasification in the Tarakan Power System. The proposed framework combined an empirical fuel oil consumption model, a fuel-constrained available-capacity model, a conditional LNG intervention model, and probabilistic representations of pipeline natural gas supply, peak demand, PLTD available capacity, and PLTMG available capacity. Unlike conventional before-and-after comparisons, the framework applied Common Random Numbers (CRN) so that the baseline scenario without LNG regasification and the intervention scenario with LNG regasification were evaluated under identical realizations of uncertainty. This controlled, ceteris paribus comparison reduced the influence of unrelated random variation and enabled differences between the two scenarios to be more directly attributed to the LNG intervention. The working hypothesis was that conditional LNG regasification, when evaluated together with actual generation availability and gas-utilization constraints, would reduce aggregate fuel oil consumption and improve generation adequacy.

Accordingly, this study aimed to quantify the role of LNG regasification in reducing fuel oil consumption and improving the reliability of the Tarakan Power System. A data-driven Monte Carlo simulation with 10,000 iterations was used to compare the baseline and LNG intervention scenarios. The principal stochastic input variables were pipeline natural gas supply, peak demand, PLTD available capacity, and PLTMG available capacity. The analysis evaluated fuel oil consumption, available generation capacity, reserve margin, operating status, and Loss of Load Probability (LOLP), while sensitivity analysis was performed to identify the variables exerting the greatest influence on fuel oil consumption and system adequacy. Through this approach, the study provides an operational and probabilistic assessment of LNG regasification as a primary energy buffer in an isolated power system.

METHOD

Research Design and Study Area

This study employed a quantitative simulation design to evaluate the effects of liquefied natural gas (LNG) regasification on fuel oil consumption and generation adequacy in the Tarakan Power System, North Kalimantan, Indonesia. The system operated independently of the regional electricity grid and was supplied by diesel power plants (Pembangkit Listrik Tenaga Diesel, PLTD) and gas-engine power plants (Pembangkit Listrik Tenaga Mesin Gas, PLTMG).

A data-driven, non-sequential Monte Carlo simulation was performed at the aggregate system level using a daily time resolution (Abud et al., 2023; Singh et al., 2022). Two scenarios were evaluated: a baseline scenario without LNG regasification and an intervention scenario with conditional LNG supply. Common Random Numbers (CRN) were applied so that both scenarios were evaluated under identical stochastic conditions, enabling the effects of the LNG intervention to be compared on a controlled ceteris paribus basis.

Data Sources and Research Variables

This study used secondary daily operational data from the Tarakan isolated power system. The baseline period covered January 1–September 13, 2025, comprising 256 daily observations, whereas the routine LNG-operation period covered October 10, 2025–April 15, 2026, comprising 188 daily observations. The 26-day commissioning period from September 14 to October 9, 2025, was excluded because it did not represent regular operating conditions. The baseline and routine LNG-operation records were combined to estimate the common empirical distributions of pipeline gas supply and peak load and to calibrate the fuel oil consumption model applied to both scenarios. PLTD and PLTMG available-capacity records covered June 9, 2025–April 15, 2026, comprising 311 daily observations.

The data were obtained from daily generation operating reports, system power-balance reports, and generating-unit operational records. All records that met the completeness, consistency, and operational-plausibility criteria were used and aligned by operating date. Gas quantities were expressed in billion British thermal units per day (BBTUD). The variables, units, observation periods, and numbers of observations used in the model are summarized in Table 1.

Table 1. Data Used in the Study

Variable	Unit	Observation Period	Calendar-Day Coverage	Function in the Model
Pipeline gas supply	BBTUD	Jan. 1, 2025–Apr. 15, 2026, excluding the commissioning period	444 days	Stochastic primary-energy input
LNG regasification supply	BBTUD	Oct. 10, 2025–Apr. 15, 2026	188 days	Historical basis for the conditional LNG-intervention model
Daily peak load	MW	Jan. 1, 2025–Apr. 15, 2026, excluding the commissioning period	444 days	Stochastic demand input
PLTD available capacity	MW	June 9, 2025–Apr. 15, 2026	311 days	Available oil-fired generation capacity
PLTMG available capacity	MW	June 9, 2025–Apr. 15, 2026	311 days	Available gas-fired generation capacity

Fuel oil consumption	kL/day	Jan. 1, 2025–Apr. 15, 2026, excluding the commissioning period	444 days	Regression response variable and simulation output
Actual system available capacity	MW	June 9, 2025–Apr. 15, 2026	311 days	Parameter estimation and model-validation target
Operating status	Category	June 9, 2025–Apr. 15, 2026, excluding the commissioning period	285 days	Model validation and generation-adequacy assessment

Data Preprocessing and Probability Distribution Modeling

Data preprocessing included standardizing decimal notation, converting date fields into a consistent format, aligning observations by operating date, and screening missing, nonnumeric, or operationally implausible values. For the LNG-operation period, pipeline gas supply was obtained by separating the recorded LNG contribution from the reported total daily gas supply.

The probability distributions of pipeline gas supply, daily peak load, PLTD available capacity, and PLTMG available capacity were estimated using Kernel Density Estimation (KDE). KDE was selected because operational data may exhibit asymmetric, multimodal, or tail behavior that cannot always be adequately represented by a predetermined parametric distribution. This approach preserves the empirical characteristics of the historical data without imposing normality or another fixed distributional form (Giannelos et al., 2025). For a historical sample $x_1, x_2, \dots, x_n$, the estimated probability density was expressed as

$$\hat{f}_h(x) = \frac{1}{nh}\sum_{j=1}^{n} K\left(\frac{x-x_j}{h}\right), \quad (1)$$

where $\hat{f}_h(x)$ is the estimated probability density, $n$is the number of historical observations, $K(\cdot)$ is the Gaussian kernel, and $h$is the bandwidth determined using Scott's rule.

Samples generated for daily peak load, PLTD available capacity, and PLTMG available capacity were restricted to their respective historical operating ranges using

$$x_i^* = \min[\max(x_i, L_x), U_x], \quad (2)$$

where x_i is the value generated from the KDE distribution, while L_x and U_x are the corresponding lower and upper historical bounds. This clipping procedure prevented negative values and values exceeding the observed operating ranges. Pipeline gas supply was sampled directly from its KDE distribution without clipping to preserve its empirical variability. The generated input samples were checked against the historical descriptive statistics and histogram–KDE patterns to ensure that the principal distributional characteristics were retained.

Monte Carlo Simulation and Scenario Design

The Monte Carlo simulation comprised 10,000 iterations. In each iteration, pipeline gas supply, daily peak load, PLTD available capacity, and PLTMG available capacity were sampled from their respective empirical marginal distributions. Through the Common Random Numbers procedure, the same stochastic realizations were used in both scenarios. LNG supply was set to zero in the baseline scenario, whereas the intervention scenario incorporated the conditional LNG supply described in the following section. The overall simulation and scenario-comparison framework is presented in Figure 1.

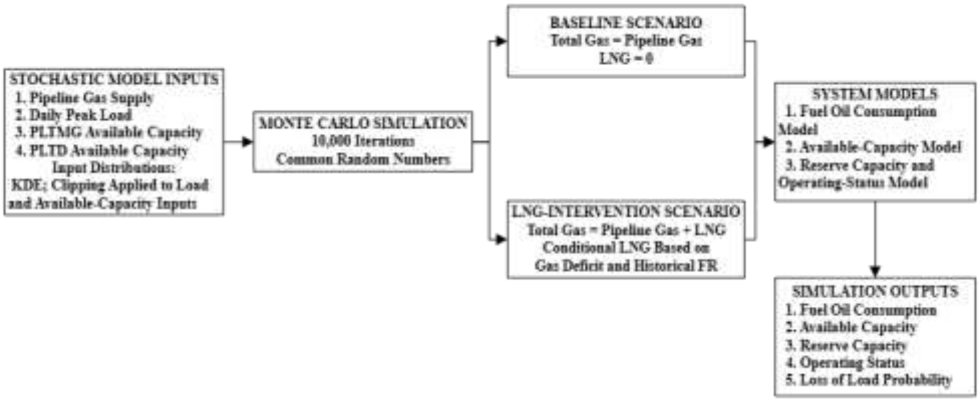

Figure 1. Monte Carlo Simulation and Scenario-Comparison Framework

All computations were implemented in Python using the Google Colab environment. Data processing was performed using pandas, numerical computation and random sampling using NumPy, Ordinary Least Squares regression using statsmodels, and Gaussian KDE using SciPy. A fixed random seed of 42 was applied to ensure the reproducibility of the 10,000 simulation iterations.

Conditional LNG Intervention Model

LNG was modeled as a conditional supplement to pipeline gas. An empirical gas-to-capacity factor was first derived to estimate the gas requirement associated with PLTMG available capacity. Because the historical records did not separately report the gas-supported PLTMG contribution, it was estimated as the difference between total system available capacity and PLTD available capacity:

$$\gamma_j = \frac{P_{\text{avail},j}^{\text{hist}} - A_{\text{D},j}^{\text{hist}}}{Q_{\text{tot},j}^{\text{hist}}}, \tag{3}$$

where $P_{\text{avail},j}^{\text{hist}}$ is historical system available capacity, $A_{\text{D},j}^{\text{hist}}$ is historical PLTD available capacity, and $Q_{\text{tot},j}^{\text{hist}}$ is the corresponding daily gas realization.

After invalid and infinite ratios were removed, a Gaussian KDE was fitted to the valid ratios and evaluated over a 1,000-point grid. The continuous mode of the distribution was used as the representative gas-to-capacity factor:

$$\gamma_g = \arg\max_{\gamma} \hat{f}_\gamma(\gamma) = 4.6720 \text{ MW/BBTUD}. \tag{4}$$

This factor represents an empirical daily-scale relationship rather than an instantaneous thermodynamic efficiency. The maximum gas absorption supported by the sampled PLTMG available capacity was calculated as

$$Q_{\text{G},i}^{\max} = \frac{A_{\text{G},i}}{\gamma_g}, \tag{5}$$

and the corresponding pipeline gas deficit was

$$D_i = \max\left(0, Q_{\text{G},i}^{\max} - Q_{\text{pipe},i}\right). \tag{6}$$

Historical LNG fulfillment was represented using the Fulfillment Ratio:

$$FR_j = \frac{Q_{\text{LNG},j}^{\text{hist}}}{D_j^{\text{hist}}}, \qquad D_j^{\text{hist}} > 0.01 \text{ BBTUD}, \tag{7}$$

where the threshold excluded negligible deficit values. Only records from routine LNG operation beginning on October 10, 2025, were used. This criterion yielded 164 historical FR observations for stratified bootstrapping.

To retain the historical relationship between deficit magnitude and LNG fulfillment, the observations were divided into low-, medium-, and high-deficit strata using the 33.33rd and 66.67th percentiles. For each simulated deficit, an FR value was sampled with replacement from the corresponding historical stratum:

$$FR_i \sim \{FR_j \mid j \in S_k\}, \tag{8}$$

where S_k denotes the FR observations associated with deficit stratum k.
The simulated LNG supply was then calculated as

$$Q_{\mathrm{LNG},i} = \begin{cases} 0, & D_i \leq 0, \\ \min(D_i FR_i, Q_{\mathrm{LNG}}^{\max}), & D_i > 0, \end{cases} \tag{9}$$

where $Q_{\mathrm{LNG}}^{\max} = 2.8123$ BBTUD, corresponding to the maximum daily LNG supply observed in the historical intervention dataset. This formulation activated LNG only during a pipeline gas deficit, retained historical fulfillment behavior, and limited the simulated supply to the highest observed daily realization.

Fuel Oil Consumption Model

Daily fuel oil consumption was represented using an aggregate surrogate model for the Tarakan generation system rather than the Specific Fuel Consumption of individual PLTD units. This approach provides an efficient representation of system-level operational relationships for repeated simulation (Lim et al., 2025).

Total gas supply in iteration i was calculated as

$$Q_{\mathrm{tot},i} = Q_{\mathrm{pipe},i} + Q_{\mathrm{LNG},i}, \tag{10}$$

where $Q_{\mathrm{LNG},i} = 0$ in the baseline scenario. Because the available gas could exceed the amount utilized by the PLTMG fleet, absorbed gas was limited to

$$Q_{\mathrm{abs},i} = \min\left(Q_{\mathrm{tot},i}, Q_{\mathrm{G},i}^{\max}\right). \tag{11}$$

Fuel oil consumption was estimated using Multiple Linear Regression with coefficients obtained through Ordinary Least Squares from historical daily peak load, total gas realization, and fuel oil consumption. The calibrated model was

$$F_i = \max\left[0, 54.9575 + 4.8938L_i - 30.0347Q_{\mathrm{abs},i}\right], \tag{12}$$

where F_i is estimated fuel oil consumption in kL/day, L_i is daily peak load in MW, and $Q_{\mathrm{abs},i}$ is absorbed gas in BBTUD. The multivariable formulation represents the simultaneous relationship of system demand and gas utilization with fuel oil consumption (Sias et al., 2024).

Historical total gas realization was used to estimate the regression coefficients, whereas the simulation applied the gas-absorption constraint to represent the amount that could be utilized by the available PLTMG fleet. The fitted mean response was used in each iteration without separately resampling the regression residuals, thereby maintaining the focus on operational input uncertainty and the paired effect of LNG regasification.

Fuel-Constrained Available Capacity Model

System available capacity was estimated by considering both technical generating capacity and gas-supply constraints. The PLTD contribution was represented directly by its sampled available capacity because fuel oil availability was not modeled as a stochastic capacity constraint. In contrast, usable PLTMG capacity was limited by both its sampled available capacity and the capacity supported by total gas supply:

$$P_{\mathrm{G},i} = \min\left(A_{\mathrm{G},i}, \gamma_g Q_{\mathrm{tot},i}\right), \tag{13}$$

where $P_{\mathrm{G},i}$ is usable PLTMG capacity, $A_{\mathrm{G},i}$ is sampled PLTMG available capacity, and $\gamma_g Q_{\mathrm{tot},i}$ is the capacity supported by the daily gas realization.

Total system available capacity was then calculated as

$$P_{\mathrm{avail},i} = A_{\mathrm{D},i} + P_{\mathrm{G},i}, \tag{14}$$

where $A_{\mathrm{D},i}$ is sampled PLTD available capacity. This formulation prevents PLTMG output from exceeding either its technical available capacity or the capacity supported by the available gas.

Reliability Assessment

Reliability was assessed in terms of generation adequacy, namely the ability of available generation to meet daily peak load under uncertain operating conditions (Tillmanns et al., 2026). Reserve capacity was calculated as

$$R_i = P_{\mathrm{avail},i} - L_i, \tag{15}$$

where R_i is reserve capacity in MW, $P_{\mathrm{avail},i}$ is total system available capacity, and L_i is daily peak load. Operating status was classified using a 4.5 MW reserve threshold, corresponding to the capacity of the largest generating unit:

$$S_i = \begin{cases} \text{Deficit}, & R_i < 0, \\ \text{Alert}, & 0 \le R_i \le 4.5, \\ \text{Normal}, & R_i > 4.5. \end{cases} \tag{16}$$

Loss of Load Probability (LOLP) was estimated as the proportion of iterations with negative reserve capacity:

$$LOLP = \frac{1}{N}\sum_{i=1}^{N} I\,(R_i < 0), \tag{17}$$

where $N = 10{,}000$, and $I(\cdot)$ equals one when the condition is satisfied and zero otherwise.

Model Validation

The conditional LNG intervention model was validated through *in-sample historical backtesting* of the Fulfillment Ratio (FR). Historical and simulated FR distributions were compared using their means, standard deviations, and first-order Wasserstein Distance:

$$W_1 = \int_0^1 \left|F^{-1}_{\mathrm{FR,hist}}(u) - F^{-1}_{\mathrm{FR,sim}}(u)\right| \, du, \tag{18}$$

where $F^{-1}_{\mathrm{FR,hist}}(u)$ and $F^{-1}_{\mathrm{FR,sim}}(u)$ are the empirical quantile functions of the historical and simulated FR distributions, respectively. A study-specific acceptance threshold of $W_1 \le 0.05$ was adopted.

The fuel oil consumption and available-capacity models were evaluated using Mean Absolute Percentage Error (MAPE), while the fuel oil model was additionally assessed using the coefficient of determination (R^2):

$$MAPE = \frac{100}{n}\sum_{j=1}^{n}\left|\frac{y_j - \hat{y}_j}{y_j}\right|, \tag{19}$$

where y_j and $\hat{y}_j$ are the historical and estimated values. The interpretation of R^2 followed Hair et al. (2021), whereas MAPE followed Lewis (1982): values below 10% indicated highly accurate estimates, 10%–20% good estimates, 20%–50% reasonable estimates, and above 50% inaccurate estimates. A MAPE not exceeding 20% was adopted as the acceptance criterion.

The available-capacity model was further evaluated using a confusion matrix for deficit and nondeficit conditions. Classification accuracy was calculated as

$$Accuracy = \frac{TP+TN}{TP+TN+FP+FN}, \tag{20}$$

where TP, TN, FP, and FN denote true-positive, true-negative, false-positive, and false-negative classifications, respectively (Han et al., 2022). An accuracy of at least 85% was considered satisfactory (Congalton & Green, 2019), with particular attention given to false-negative cases.

Statistical and Sensitivity Analysis

The baseline and LNG-intervention outputs were summarized using descriptive statistics, including the mean, standard deviation, minimum, maximum, median, and selected percentiles. Because the Common Random Numbers procedure produced paired observations, changes in fuel oil consumption, available capacity, and reserve capacity were evaluated using iteration-level differences between the two scenarios.

The upper distribution of fuel oil consumption was assessed using the 90th and 95th percentiles, Conditional Value at Risk at the 90% level ($CVaR_{90}$), and empirical exceedance probabilities. $CVaR_{90}$ represented the mean consumption among outcomes at or above the 90th percentile, while exceedance probability was calculated as

$$\hat{P}(F_s > x) = \frac{1}{N}\sum_{i=1}^{N} I\left(F_{s,i} > x\right), \tag{21}$$

where $F_{s,i}$ is fuel oil consumption in scenario s, and x is the selected threshold. Generation adequacy was compared using the distributions of available capacity and reserve capacity, operating-status frequencies, and LOLP.

Sensitivity analysis was conducted using a One-at-a-Time (OAT) approach around the historical mean of each stochastic input. Pipeline gas supply, peak load, PLTD available capacity, and PLTMG available capacity were individually varied by $\pm 10\%$, while the remaining inputs were maintained at their mean values:

$$x^- = 0.90\overline{x}, \qquad x^+ = 1.10\overline{x}. \tag{22}$$

The sensitivity range was calculated as

$$S_x = Y_{x,+10\%} - Y_{x,-10\%}, \tag{23}$$

where Y denotes fuel oil consumption or reserve capacity. A larger absolute value of S_x indicated a stronger influence of the corresponding input. The relative sensitivities under the baseline and LNG-intervention scenarios were presented using tornado diagrams.

RESULTS AND DISCUSSION

Model Validation

The simulated input distributions retained the principal characteristics of the historical operating data. The mean pipeline gas supply was 5.6030 BBTUD in the historical data and 5.5964 BBTUD in the simulated data. Historical and simulated daily peak loads had the same mean of 49.21 MW, while the corresponding means for PLTD available capacity were both 35.67 MW. The historical and simulated means of PLTMG available capacity were also closely aligned at 30.11 and 30.10 MW, respectively. Comparisons of medians, standard deviations, and selected percentiles similarly showed only minor differences, indicating that the KDE-generated inputs adequately represented the observed operating variability.

The validation results for the input distributions, conditional LNG intervention, fuel oil consumption model, and available-capacity model are summarized in Table 2. The historical and simulated Fulfillment Ratio distributions had similar central tendencies and dispersion. Their mean difference was only 0.69 percentage points, while the difference in standard deviation was 0.0315. The Wasserstein Distance of 0.013673 was substantially below the specified threshold of 0.05, confirming that the stratified conditional bootstrap retained the overall historical fulfillment pattern rather than merely reproducing its mean.

Table 2. Summary of Model Validation Results

Model Component	Validation Indicator	Result	Assessment
Pipeline gas distribution	Historical/simulated mean	5.6030/5.5964 BBTUD	Closely aligned
Peak-load distribution	Historical/simulated mean	49.21/49.21 MW	Closely aligned
PLTD available-capacity distribution	Historical/simulated mean	35.67/35.67 MW	Closely aligned
PLTMG available-capacity distribution	Historical/simulated mean	30.11/30.10 MW	Closely aligned
Conditional LNG intervention	Historical/simulated mean FR	89.87%/90.56%	Closely aligned
Conditional LNG intervention	Historical/simulated FR standard deviation (percentage points)	1.1517/1.1832	Closely aligned
Conditional LNG intervention	Wasserstein Distance	0.013673	Below the 0.05 threshold
Fuel oil consumption model	R^2	0.8311	Strong explanatory ability
Fuel oil consumption model	MAPE	11.23%	Good accuracy
Available-capacity model	MAPE	2.29%	Highly accurate
Available-capacity model	Classification accuracy	98.95%	Satisfactory
Available-capacity model	False negatives	0	All historical deficits detected

The fuel oil consumption model explained 83.11% of the historical variation in daily fuel use and achieved a MAPE of 11.23%. This result indicates that peak load and gas utilization captured most of the aggregate variation in fuel oil consumption, although operational factors not explicitly represented in the model—such as unit-specific fuel efficiency, dispatch patterns, and start-stop behavior—continued to account for part of the remaining variation.

The available-capacity model produced a MAPE of 2.29%, indicating close agreement with historical system available capacity. It also correctly identified both historical deficit observations and produced no false-negative classifications. Three nondeficit observations were conservatively classified as deficits, resulting in an overall accuracy of 98.95%. Although this performance supports the use of the model for scenario analysis, the classification result should be interpreted in light of the limited number of historical deficit observations.

Fuel Oil Consumption

The simulated fuel oil consumption statistics for the baseline and LNG-intervention scenarios are presented in Table 3. As shown in Table 3, LNG regasification reduced average fuel oil consumption from 133.33 to 113.51 kL/day. The reduction of 19.82 kL/day, or 14.87%, demonstrates that additional gas enabled a larger proportion of system demand to be supplied by the PLTMG fleet, thereby reducing the requirement for oil-fired generation.

Table 3. Daily Fuel Oil Consumption under the Baseline and LNG-Intervention Scenarios

Statistic	Baseline (kL/day)	LNG Intervention (kL/day)	Difference (kL/day)	Change
Mean	133.33	113.51	−19.82	−14.87%
Standard deviation	32.65	29.10	−3.55	−10.87%
P10	92.65	76.03	−16.62	−17.94%
Median	131.66	113.49	−18.17	−13.80%
P90	176.39	151.44	−24.95	−14.14%
P95	188.98	161.48	−27.50	−14.55%
$CVaR_{90}$	192.77	164.88	−27.89	−14.47%
Maximum	249.12	235.25	−13.87	−5.57%

The reduction was not confined to the mean. Median consumption declined from 131.66 to 113.49 kL/day, showing that the effect remained evident under typical operating conditions. Consumption also declined across the lower and upper parts of the distribution. P90 decreased by 24.95 kL/day, P95 decreased by 27.50 kL/day, and $CVaR_{90}$ decreased by 27.89 kL/day. These changes indicate that LNG regasification was particularly effective in reducing fuel oil use during operating conditions associated with high oil consumption.

The changes in the fuel oil probability distribution and exceedance probability are presented in Figure 2.

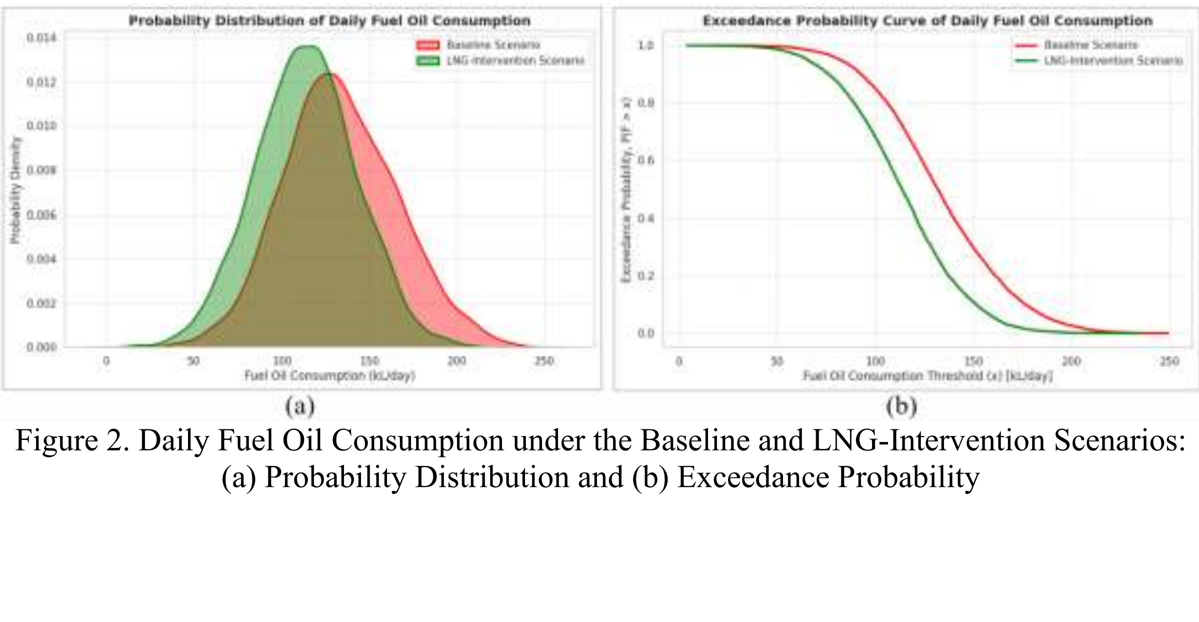

(a) (b)

Figure 2. Daily Fuel Oil Consumption under the Baseline and LNG-Intervention Scenarios: (a) Probability Distribution and (b) Exceedance Probability

The probability distribution shifted to the left under the LNG-intervention scenario, with a greater concentration of outcomes at lower consumption levels. Consistent with this shift, the intervention exceedance curve remained below the baseline curve across most consumption thresholds. Thus, for the same fuel oil threshold, the probability of exceeding that value was lower when conditional LNG regasification was available.

The paired CRN comparison produced a mean fuel oil saving of 19.82 kL/day and a median saving of 13.57 kL/day. Positive savings occurred in 67.15% of the iterations, while P90 savings reached 54.06 kL/day. The fact that savings were not observed in every iteration is consistent with the conditional structure of the intervention. LNG was not activated when pipeline gas was already sufficient, and its benefits were limited when PLTMG available capacity could not absorb the additional gas. Consequently, the results do not imply that a fixed LNG volume produces a uniform reduction in fuel oil use; rather, the benefit depends on the interaction among gas deficit, LNG fulfillment, load, and PLTMG readiness.

Generation Adequacy and Reliability Performance

The effects of LNG regasification on available capacity and reserve capacity are summarized in Table 4.

Table 4. Available Capacity and Reserve Capacity under the Baseline and LNG-Intervention Scenarios

Indicator	Statistic	Baseline (MW)	LNG Intervention (MW)	Difference (MW)
Available capacity	Mean	60.94	64.02	+3.08
Available capacity	Standard deviation	4.46	3.83	−0.63
Available capacity	Minimum	43.38	48.49	+5.11
Available capacity	P10	54.94	59.00	+4.06
Reserve capacity	Mean	11.73	14.81	+3.08
Reserve capacity	Minimum	−7.76	−4.36	+3.40
Reserve capacity	P10	4.27	8.08	+3.81

Average system available capacity increased from 60.94 to 64.02 MW, equivalent to an improvement of 3.08 MW or 5.05%. The minimum available capacity increased by 5.11 MW, while P10 increased from 54.94 to 59.00 MW. These lower-tail improvements indicate that LNG produced its most consequential capacity benefit when pipeline gas would otherwise have constrained PLTMG utilization.

Average reserve capacity increased by the same absolute amount, from 11.73 to 14.81 MW. More importantly, P10 reserve capacity increased from 4.27 to 8.08 MW. Under the baseline scenario, the P10 value was slightly below the 4.5 MW N−1-oriented reserve threshold. Following the LNG intervention, the P10 value exceeded that threshold, indicating that the lower portion of the reserve distribution moved into a more secure operating range.

The probability distributions of reserve capacity under the two scenarios are shown in Figure 3. The intervention distribution shifted to the right, showing a higher probability of larger reserve capacity. The probability mass below the 0 MW deficit boundary was also considerably smaller. Nevertheless, the minimum reserve remained negative at −4.36 MW, compared with −7.76 MW under the baseline scenario. Regasification therefore reduced both the frequency and depth of deficit conditions but did not eliminate the possibility of a deficit under all combinations of peak load and generation availability.

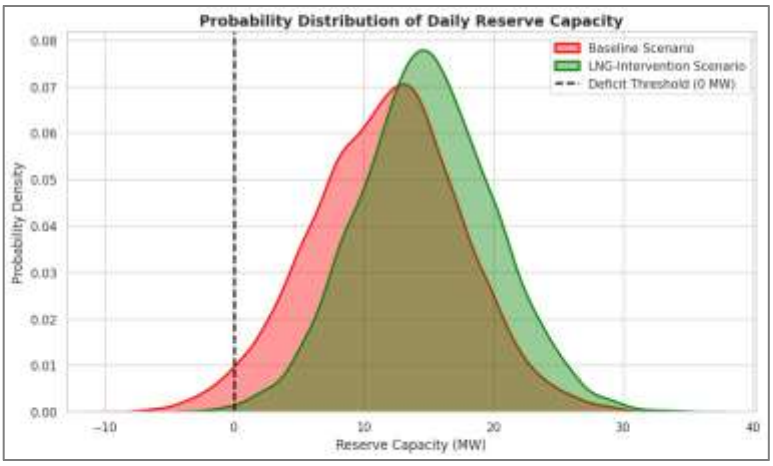

Figure 3. Probability Distribution of Daily Reserve Capacity under the Baseline and LNG-Intervention Scenarios

The resulting changes in operating status are presented in Table 5.

Table 5. Operating Status under the Baseline and LNG-Intervention Scenarios

Operating Status	Baseline Iterations	Baseline Share	LNG-Intervention Iterations	Intervention Share	Change
Normal	8,933	89.33%	9,772	97.72%	+839
Alert	841	8.41%	207	2.07%	−634
Deficit	226	2.26%	21	0.21%	−205
Total	10,000	100.00%	10,000	100.00%	—

Table 5 shows that the proportion of normal operating conditions increased from 89.33% to 97.72%. Most of this improvement resulted from the movement of alert conditions into the normal category, as the number of alert iterations declined from 841 to 207. The number of deficit iterations decreased from 226 to 21.

Because LOLP was calculated as the proportion of deficit iterations, it decreased from 2.26% under the baseline scenario to 0.21% under the LNG-intervention scenario. This represents a reduction of 2.05 percentage points, or approximately 90.71% relative to the baseline risk. The reduction confirms that additional gas can improve generation adequacy by converting otherwise unavailable PLTMG capacity into usable system capacity.

However, the 21 remaining deficit iterations demonstrate that primary-energy reinforcement alone cannot guarantee adequacy under every operating condition. Deficits may still occur when high peak load coincides with low PLTD or PLTMG available capacity, or when the available PLTMG fleet cannot fully convert additional gas into electrical capacity. The reliability benefit of LNG must therefore be understood as a substantial risk reduction rather than the complete removal of generation risk.

Sensitivity Analysis

The OAT sensitivity results for fuel oil consumption are presented in Figure 4. The dashed reference lines represent the baseline values of 133.3 kL/day for the baseline scenario and 113.5 kL/day for the LNG-intervention scenario.

Peak load was the most influential variable in both scenarios. A ±10% variation in peak load produced fuel oil consumption ranges of 109.2–157.4 kL/day in the baseline scenario and 89.4–137.6 kL/day in the LNG-intervention scenario. Although LNG shifted the overall level of fuel oil consumption downward, peak load remained the dominant driver of fuel use because increasing demand required greater utilization of oil-fired generation when gas-fired capacity was insufficient to meet the additional load.

Pipeline gas supply was the second most influential variable in the baseline scenario, producing a fuel oil consumption range of 123.3–146.4 kL/day. Under the LNG-intervention scenario, this range narrowed substantially to 110.0–118.5 kL/day. This reduction indicates that conditional LNG supply buffered part of the effect of pipeline gas fluctuations by supplying additional gas when pipeline availability was insufficient, thereby reducing the system's dependence on oil-fired generation.

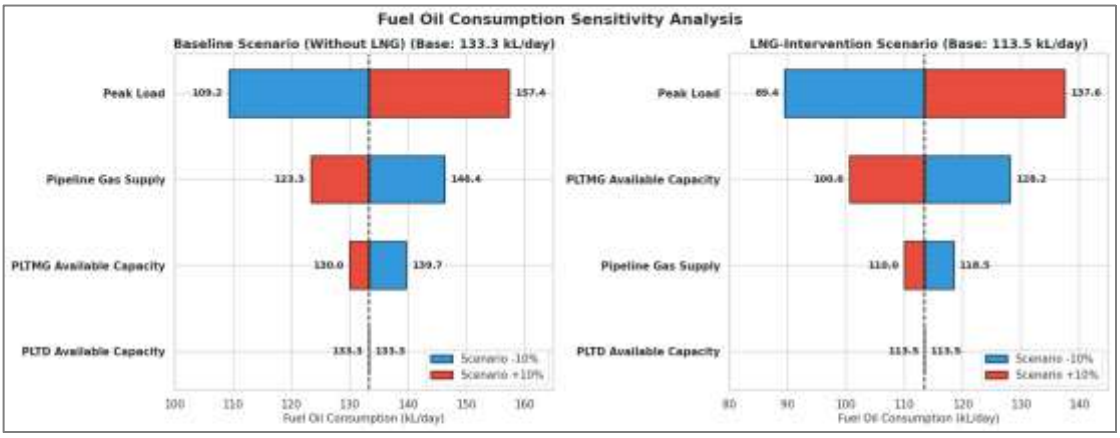

Figure 4. Tornado Diagrams of Fuel Oil Consumption Sensitivity under the Baseline and LNG-Intervention Scenarios

Conversely, the influence of PLTMG available capacity became considerably stronger after LNG was introduced. Variations in PLTMG available capacity produced fuel oil consumption ranges of 130.0–139.7 kL/day in the baseline scenario and 100.6–128.2 kL/day in the LNG-intervention scenario. This result indicates that the benefits of additional LNG increasingly depended on the technical readiness of the PLTMG fleet, because the supplied gas could reduce fuel oil consumption only when sufficient gas-engine capacity was available to absorb and utilize it.

The OAT sensitivity results for reserve capacity are shown separately in Figure 5. The reference reserve values were approximately 11.7 MW in the baseline scenario and 14.8 MW in the LNG-intervention scenario.

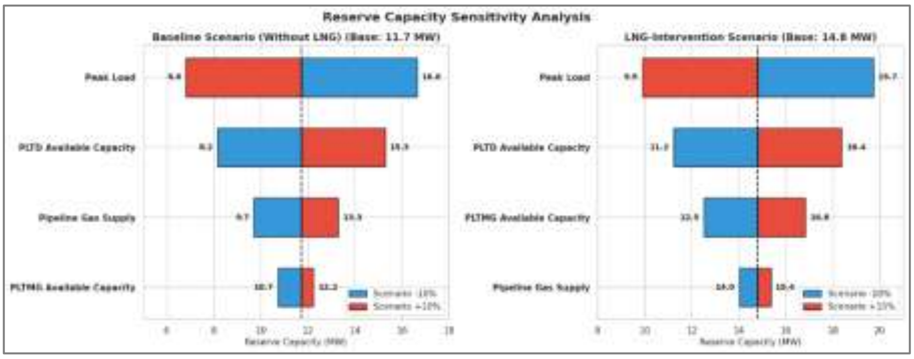

Figure 5. Tornado Diagrams of Reserve Capacity Sensitivity under the Baseline and LNG-Intervention Scenarios

Peak load was also the dominant determinant of reserve capacity. A ±10% variation generated reserve-capacity ranges of 6.8–16.6 MW under the baseline scenario and 9.9–19.7

MW under the LNG-intervention scenario. LNG increased the overall reserve level but did not remove the direct adverse effect of increasing demand on the system capacity margin.

PLTD available capacity remained the second most influential variable, producing reserve ranges of 8.2–15.3 MW in the baseline scenario and 11.2–18.4 MW in the intervention scenario. This result confirms that PLTD continued to provide an important adequacy contribution even when LNG reduced the system's dependence on fuel oil.

The sensitivity of reserve capacity to PLTMG available capacity increased from 10.7–12.2 MW under the baseline scenario to 12.5–16.8 MW under the intervention scenario. In contrast, the effect of pipeline gas supply narrowed from 9.7–13.3 MW to 14.0–15.4 MW. These results indicate that LNG shifted the principal constraint affecting gas-fired generation: the system became less sensitive to pipeline gas fluctuations but more dependent on maintaining adequate PLTMG available capacity.

Although the reserve-capacity responses were approximately linear within the ±10% range, their effects on operating status and LOLP remained threshold-dependent. A relatively small change in reserve capacity may not alter system status when the reserve is sufficiently high, but it may change the classification when the reserve approaches either the 0 MW deficit boundary or the 4.5 MW normal-operation threshold.

Operational Implications of LNG Regasification

The findings show that LNG regasification functioned as a conditional primary-energy buffer rather than as a replacement for pipeline gas. Pipeline gas remained the principal gaseous fuel source, while LNG was introduced only when pipeline supply was insufficient and the available PLTMG fleet could utilize additional gas. This mechanism ensured that LNG deployment followed actual system requirements rather than being treated as a constant supply.

The resulting *fuel switching* occurred at the system level by shifting part of the generation requirement from oil-fired PLTD units to gas-fired PLTMG units. Higher absorbed-gas utilization reduced the need for PLTD operation and made additional PLTMG capacity usable that would otherwise have remained constrained by insufficient primary-energy supply.

This mechanism produced simultaneous improvements in operational efficiency and generation adequacy. Average fuel oil consumption declined by 14.87%, while available capacity, reserve capacity, the proportion of normal operating conditions, and LOLP all improved. The results therefore indicate that reducing fuel oil dependence did not create a trade-off with reliability; instead, more effective utilization of the available gas-fired fleet improved both operational efficiency and reliability.

The sensitivity analysis shows that these benefits depend on broader operating conditions. LNG reduced exposure to pipeline gas fluctuations, but peak load remained the dominant pressure on fuel consumption and reserve capacity, while PLTMG readiness became increasingly important after the intervention. Effective LNG utilization should therefore be supported by peak-load management, preventive maintenance of PLTMG units, continued PLTD readiness, and reliable pipeline gas operation. Overall, the findings support the hypothesis that conditional LNG regasification can serve as an operational flexibility resource that reduces fuel oil consumption and strengthens the reliability of an isolated power system.

CONCLUSION

This study developed a data-driven probabilistic framework to evaluate the role of liquefied natural gas (LNG) regasification in the Tarakan isolated power system. The framework integrated empirical stochastic input variables, a conditional LNG intervention model, an aggregate fuel oil consumption model, and a fuel-constrained available-capacity model within a 10,000-iteration Monte Carlo simulation using Common Random Numbers (CRN). The fuel oil consumption model achieved a coefficient of determination (R^2) of 0.8311 and a Mean Absolute Percentage Error (MAPE) of 11.23%. The available-capacity model achieved a MAPE of 2.29%, while the operating status predicted from its estimates was classified with an accuracy of 98.95%.

Compared with the baseline scenario, LNG regasification reduced average fuel oil consumption from 133.33 to 113.51 kL/day, representing a reduction of 19.82 kL/day (14.87%). It also increased the average available generation capacity from 60.94 to 64.02 MW and the average reserve margin from 11.73 to 14.81 MW, while reducing the Loss of Load Probability (LOLP) from 2.26% to 0.21%. These results demonstrate that conditional LNG supply can simultaneously reduce dependence on fuel oil while improving generation adequacy and overall system reliability.

The sensitivity analysis showed that peak demand remained the dominant factor influencing fuel oil consumption and the reserve margin. LNG regasification reduced the system's sensitivity to fluctuations in pipeline natural gas supply, whereas PLTMG available capacity became increasingly influential because the additional natural gas improved system performance only when sufficient gas-engine generating capacity was available to utilize it. Therefore, LNG regasification should be regarded as a conditional primary energy buffer and a source of operational flexibility that supports system-level fuel switching, enhances the utilization of gas-fired generation, and strengthens the reliability of isolated power systems with similar operating characteristics.

REFERENCES

Abud, T. P., Augusto, A. A., Fortes, M. Z., Maciel, R. S., & Borba, B. S. M. C. (2023). State of the art Monte Carlo method applied to power system analysis with distributed generation. *Energies*, *16*(1), Article 394. https://doi.org/10.3390/en16010394

Adi, T. W. (2023). Influence of fuel price, electricity price, fuel consumption on operating cost, generation and operating income: A case study on PLN. *International Journal of Energy Sector Management*, *17*(2), 227–250. https://doi.org/10.1108/IJESM-07-2021-0008

Congalton, R. G., & Green, K. (2019). *Assessing the accuracy of remotely sensed data: Principles and practices* (3rd ed.). CRC Press.

Giannelos, S., Pudjianto, D., Zhang, T., & Strbac, G. (2025). Energy hub operation under uncertainty: Monte Carlo risk assessment using Gaussian and KDE-based data. *Energies*, *18*(7), Article 1712. https://doi.org/10.3390/en18071712

Hair, J. F., Hult, G. T. M., Ringle, C. M., & Sarstedt, M. (2021). *A primer on partial least squares structural equation modeling (PLS-SEM)* (3rd ed.). SAGE Publications.

Han, J., Pei, J., & Tong, H. (2022). *Data mining: Concepts and techniques* (4th ed.). Morgan Kaufmann.

Lai, C. S., Yan, M., Li, X., Lai, L. L., & Xu, Y. (2021). Coordinated operation of electricity and natural gas networks with consideration of congestion and demand response. *Applied Sciences*, *11*(11), Article 4987. https://doi.org/10.3390/app11114987

Lewis, C. D. (1982). *Industrial and business forecasting methods*. Butterworth Scientific.

Lim, Y., Son, M., Park, K., Kim, M., Song, K., Lee, H., & Kim, H. (2025). Power system decision making in the age of deep learning: A comprehensive review. *Energies*, *18*(18), Article 4867. https://doi.org/10.3390/en18184867

Machfudiyanto, R. A., Humang, W. P., Wahjuningsih, N., Kamil, I., & Putra, Y. Y. A. (2023). Probability of risk factors affecting small-scale LNG supply chain activities in the Indonesian archipelago. *Infrastructures*, *8*(4), Article 74. https://doi.org/10.3390/infrastructures8040074

Machfudiyanto, R. A., Muslim, F., Humang, W. P., Wahjuningsih, N., Kamil, I., Ichsan, M., & Putra, Y. Y. A. (2023). Optimization of the risk-based small-scale LNG supply chain in the Indonesian archipelago. *Heliyon*, *9*(8), Article e19047. https://doi.org/10.1016/j.heliyon.2023.e19047

Nallainathan, S., Arefi, A., Lund, C., & Mehrizi-Sani, A. (2025). Microgrid reliability incorporating uncertainty in weather and equipment failure. *Energies*, *18*(8), Article 2077. https://doi.org/10.3390/en18082077

Saleem, A. F., & AlMuhaini, M. (2021). Reliability assessment of an isolated hybrid microgrid using Markov modeling and Monte Carlo simulation. *Engineering Review*, *41*(2), 62–73. https://doi.org/10.30765/er.1478

Sias, Q. A., Gantassi, R., Choi, Y., & Bae, J. H. (2024). Recurrence multilinear regression technique for improving accuracy of energy prediction in power systems. *Energies*, *17*(20), Article 5186. https://doi.org/10.3390/en17205186

Singh, V., Moger, T., & Jena, D. (2022). Uncertainty handling techniques in power systems: A critical review. *Electric Power Systems Research*, *203*, Article 107633. https://doi.org/10.1016/j.epsr.2021.107633

Sommeng, A. N., Usman, & Kurnianto, J. (2023). Techno-economic and risk assessment of small-scale LNG distribution for replacing diesel fuel in Nusa Tenggara region. *International Journal of Energy Economics and Policy*, *13*(4), 356–364. https://doi.org/10.32479/ijeep.14446

Tillmanns, M., Schöttler, J., & Praktiknjo, A. (2026). A review of probabilistic resource adequacy assessments in power systems: Methods, applications, and future challenges. *Energy Policy*, *209*, Article 114924. https://doi.org/10.1016/j.enpol.2025.114924

Weng, Z., Zhou, J., & Zhan, Z. (2022). Reliability evaluation of standalone microgrid based on sequential Monte Carlo simulation method. *Energies*, *15*(18), Article 6706. https://doi.org/10.3390/en15186706

Yang, L., Wei, Z., Chen, S., Sun, G., & Zang, H. (2026). Three-stage coordinated operation of electric and natural gas systems with high penetration of renewables. *CSEE Journal of Power and Energy Systems*, *12*(2), 991–1001. https://doi.org/10.17775/CSEEJPES.2022.02620

Zhang, H., Wu, Y., Zhen, L., Jin, Y., & Wang, S. (2024). Optimization problems in liquefied natural gas transport and storage for multimodal transport companies. *Electronic Research Archive*, *32*(8), 4828–4844. https://doi.org/10.3934/era.2024221